STOKES 1.5 μm AND ANTI-STOKES 0.99 μm EMISSIONS IN Ga-Ge-Sb-S: Er[3+] AMORPHOUS CHALCOGENIDE FILMS PREPARED BY PULSED LASER DEPOSITION

Lukáš STŘIŽÍK[1a], Jiří OSWALD[b], Milan VLČEK[c], Ludvík BENEŠ[d],
Martin PAVLIŠTA[e], and Tomáš WÁGNER[a]
[a] Department of General and Inorganic Chemistry,
[b] Institute of Physics of the ASCR, v.v.i., CZ–162 00 Prague
[c] Institute of Macromolecur Chemistry of the ASCR, v.v.i.,
CZ–120 06 Prague
[d] Joint Laboratory of Solid State Chemistry,
[e] Department od Applied Physics and Mathematics,,
The University of Pardubice, CZ–532 10 Pardubice

Nowadays, rare-earth-doped materials play an important role in photonics. The reason can be seen in needs of present world for efficient data transfer, medical use, construction of modern devices and in research progress. We report the compositional dependence of Ga-Ge-Sb-S: Er[3+] pulsed laser deposited (PLD) chalcogenide films allowing the efficient Er[3+]: $^4I_{13/2} \to {}^4I_{15/2}$ (λ ≈ 1.5 μm) Stokes and Er[3+]: $^4I_{11/2} \to {}^4I_{15/2}$ (λ ≈ 0.99 μm) anti-Stokes emissions at pumping

---

[1] To whom correspondence should be addressed.

wavelengths of 980 and 1 550 nm, respectively. It was found that the lowest antimony and the highest sulphur contents in Ga-Ge-Sb-S films doped with 0.5 at. % Er^{3+} are beneficial for both mentioned emissions. The photon up-conversion emission was confidently observed in the case of PLD film with the highest content of sulphur, i.e., $(Ge_{17.8}Ga_{3.6}Sb_{3.6}S_{75})_{99.5}Er_{0.5}$. The shape of this emission band is comparable with the photon up-conversion emission observed in the bulk sample. We have also inspected the dependence of target material composition on deposition rate of the PLD. The substitution of the antimony atoms with the gallium atoms leads to lower deposition rate.

Introduction

Amorphous chalcogenides doped with rare-earth ions are promising materials in wide range of applications [1,2], such as waveguides [3], lasers [4,5], up-converters [6-8], sensors, and detectors [9,10]. The reason for this statement can be seen in the unique properties of chalcogenides, such as broad optical window range from the visible to mid-infrared spectral region, high refractive index promoting the radiative recombination probability, low phonon energy leading to a suppression of nonradiative recombination processes, and their relatively easy preparation in form of bulks and thin films [11,12]. Rare-earth ions (RE^{3+}) solubility in chalcogenide glasses can be improved; e.g., by introducing Ga(III) chalcogenides and this solubility can be higher than that of oxide glasses and even comparable with fluoride glasses [12].

Ga-Ge-Sb-S amorphous chalcogenides were also intensively studied; e.g., for infrared fibre optics [5,13,14], non-linear optics and waveguides [15,16] and, recently, we have achieved intense photon up-conversion emission from the green spectral region under various pumping wavelengths [17]. It is known that the Ga-Ge-Sb-S amorphous chalcogenides possess good solubility of RE^{3+} ions [16,18,19], exhibiting high thermal stability [16,20] and chemical resistance to moisture [21]. $Ge_{20}Ga_5Sb_{10}S_{65}$ is the intensively studied composition of Ga-Ge-Sb-S glasses [13-15,18,20-23] and there have also been studied the properties of two compositional series, i.e., $Ge_{25-x}Ga_xSb_{10}S_{65}$ (x = 0-6 at. %) and $Ge_{25-x}Ga_5Sb_{10}S_{60+x}$ (for x = 4-7 at. %) [13].

In this paper, we demonstrate the 1.5 μm Stokes (Er^{3+}: $^4I_{13/2} \rightarrow {}^4I_{15/2}$) and 0.99 μm($Er^{3+}$: $^4I_{11/2} \rightarrow {}^4I_{15/2}$) anti-Stokes emissions in Ga-Ge-Sb-S: Er^{3+} amorphous chalcogenide films prepared by the PLD technique in the dependence on chemical composition. Of interest were the compositional changes in $Ge_{25}Ga_{5+x}Sb_{5-x}S_{65}$ (x = 0, 2.5 and 4.5 at. %), $Ge_{25-x}Ga_5Sb_5S_{65+x}$ (x = 0 and 5 at. %) and, finally, $(Ge_{71.4}Ga_{14.3}Sb_{14.3})_{35-x}S_{65+x}$ (x = 0 and 10 at. %), i.e., $Ge_{25}Ga_5Sb_5S_{65}$ for x = 0 at. % and $Ge_{17.8}Ga_{3.6}Sb_{3.6}S_{75}$ for x = 10 at. %.

Experimental

Chalcogenide glasses were synthesised by the standard melt-quenching technique from high-purity elements Ge (5N), Ga (5N), Sb (5N), S (4.5N) and Er (3N) in the evacuated and sealed silica-glassy tubes at residual pressure of ~ 10^{l3} Pa. The sealed silica tubes with precisely weighted raw elements were placed into a rocking furnace and exposed to $T \approx 970$ °C with a heating rate of ≈ 1 °C min^{-1} and kept at this temperature for 24 h. Then, the melt was quenched in air, subsequently annealed at $T \approx 300$ °C for 1 h, and consequently slowly cooled down to room temperature. This step allowed us the relaxation of internal strain in glasses, thus avoiding the sample cracking. It should be noted that the $(Ge_{17.8}Ga_{3.6}Sb_{3.6}S_{75})_{99.5}Er_{0.5}$ as-prepared bulk sample could not be prepared in amorphous state.

Synthesized glasses were used as the targets for fabrication of films by the PLD technique, when the respective films were deposited onto pre-cleaned microscopic slide substrates (size 15×10×1 mm) cleaned with saponate, propan-2-ol and immersed into aqua regia (HCl : HNO$_3$ = 3 : 1) for 1 h. Finally, the substrates were rinsed with distilled water and dried by the centrifugation process. The KrF excimer laser (Lambda Physik COMPex) operated at λ = 248 nm was employed for the pulsed laser deposition. The pulse length was 30 ns with a repetition rate of 20 s^{-1} and the pulse energy of 220×10^{-3} J.

The laser spot area was ≈ 2.4 mm^2. The pressure inside the vacuum chamber before deposition was $\approx 4×10^{-4}$ Pa and during the deposition $\sim 10^{-3}$ Pa in order of magnitude. Total deposition time t was in the range of 65-100 min.

The chemical composition of target materials and films was studied using the energy dispersive X-ray (EDX) microanalyzer (IXRF System with a detector GRESHAM Sirius 10) being an integral part of a scanning electron microscope (JSM-5500 LV Jeol). Thicknesses d of deposited films, their optical band gap energies, E_g, and optical constants (refractive index, n, extinction coefficient, k) were determined with the aid of variable angle spectroscopic ellipsometry (model VASE®, J.A. Woollam, Co.) in the spectral region of 300-2300 nm with a wavelength step increment of 10 nm. The angles of light incidence onto sample surface were 65°, 70° and 75° which were close to the Brewster angle. The measured Ѱ and) parameters were fitted using the "Substrate/Film/Roughness". Optical constants of substrate were known from the previous measurement. Tauc–Lorentz parameterisation model [24,25] was used for the determination of optical constants of Ga-Ge-Sb-S: Er^{3+} films, applicable in the transparent region and interband absorption of the materials studied [24]. The surface roughness was described by effective medium approximation (EMA) according to Bruggeman [26], consisting of 50 vol. % of voids and of 50 vol. % of film material. Photoluminescence (PL) spectroscopy was used to study ≈ 1.5 μm emissions under the 980 nm laser diode pumping. In addition, we tried to observe the

Střižík L. *et al.*/Sci. Pap. Univ. Pardubice, Ser. A **21** (2015) 57–66

59

≈ 0.99 μm photon up-conversion emissions in these films when excited by the 1550 nm laser diode. The 1.5 μm PL signal was detected using the Ge detector cooled with liquid nitrogen, whereas the Si PIN diode was utilized to detect the ≈ 0.99 μm emission. The emission spectra were recorded in the spectral regions of 800-1150 and 1440-1650 nm. All measurements were carried out at room temperature.

Results and Discussion

The **A** $(Ge_{25}Ga_5Sb_5S_{65})_{99.5}Er_{0.5}$, **B** $(Ge_{25}Ga_{7.5}Sb_{2.5}S_{65})_{99.5}Er_{0.5}$, **C** $(Ge_{25}Ga_{9.5}Sb_{0.5}S_{65})_{99.5}Er_{0.5}$, **D** $(Ge_{20}Ga_5Sb_5S_{70})_{99.5}Er_{0.5}$ and **E** $(Ge_{17.8}Ga_{3.6}Sb_{3.6}S_{75})_{99.5}Er_{0.5}$ bulk chalcogenides were synthesized by procedure described in experimental part and used as targets for fabrication of films by the PLD technique. There were three compositional dependencies; namely, **A** → **B** → **C**, where antimony was replaced with gallium $(Ge_{25}Ga_{5+x}Sb_{5!x}S_{65})$, **A** → **D**, $(Ge_{25!x}Ga_5Sb_5S_{65+x})$, germanium replaced with sulphur and, finally, **A** → **E**, with the atomic ratio of cations Ge : Ga : Sb = 25 : 5 : 5 and only the total content of sulphur increased from 65 at. % to 75 at. %.

Furthermore, it was found (from EDX spectroscopy) that the chemical composition between the target material and the film deposited was changed because of sulphur depletion about ≈ 9 at. %. This behaviour was also observed in the case of the As-S and Ag-As-S chalcogenide films deposited by the pulsed laser [27-29], which can probably be related to the redeposition process during laser ablation.

The optical band gap energy, E_g, of the samples prepared has increased in the series **A** → **B** → **C** → **D** → **E** ; see Table I. It is also evident that refractive index, n, in the series **A** → **B** → **C** → **D** → **E** decreases from 2.64 to 2.36 (at $\lambda = 1\,550$ nm) as shown in Fig. 1, which is in accordance with the Moss law [30]. However, in the case of samples **A** and **B**, the dispersion of refractive index varies in a reverse order at longer wavelengths with the highest difference to be $\Delta n = 0.02$. The changes in refractive index can be explained by the particular chemical composition. When the gallium atoms are replaced with the antimony atoms in $(Ge_{25}Ga_{5+x}Sb_{5!x}S_{65})_{99.5}Er_{0.5}$, the refractive index has generally increased (**C** → **B** → **A**) due to a higher polarisability of the antimony atoms in comparison with the gallium atoms. This phenomenon is described by the Clausius–Mossotti equation [31-32] relating the refractive index with the atomic polarisability. Similar trend has also been observed in the case of samples **D** and **E** in comparison with **A**. Herein, the sulphur atoms have lower polarisability than the rest of constituent atoms and, therefore, the increase in sulphur atomic content leads to lower refractive index values.
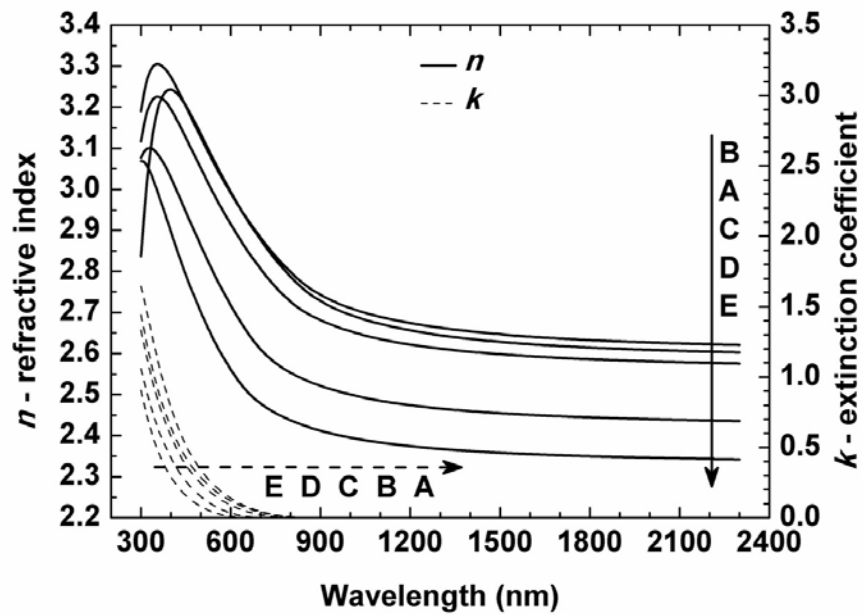
Fig. 1 Spectral dependence of the refractive index, *n*, and extinction coefficient, *k*, of PLD Ga-Ge-Sb-S: Er^{3+} films determined by fitting of the variable angle spectroscopic ellipsometry data

The deposition rate can simply be calculated as a ratio of the sample thickness, *d*, and total deposition time, *t*. All results are summarised in Table I, together with the mean squared errors (*MSE*) of ellipsometric data fit. It is possible to observe that deposition rate has tendency to decrease when the antimony atoms are replaced with the gallium atoms ($A \rightarrow B \rightarrow C$) in $Ge_{25}Ga_{5+x}Sb_{5!x}S_{65}$. Similar trends can also be observed if the germanium atoms are replaced with the sulphur atoms ($A \rightarrow D$) in $Ge_{25!x}Ga_5Sb_5S_{65+x}$ and also in the case, when the total atomic content of sulphur increases while the atomic ratio of cations remains unchanged ($A \rightarrow F$) in the $(Ge_{71.4}Ga_{14.3}Sb_{14.3})_{35!x}S_{65+x}$ structure. This behaviour can apparently be attributed to atomic polarisabilities of the substituent elements, absorption (extinction) coefficient, stoichiometry, and the structure leading to the efficient energy absorption of an excimer laser pulse by the target material.

Figure 2 shows ≈ 1.5 μm emission spectra originating from Er^{3+}: $^4I_{13/2} \rightarrow {}^4I_{15/2}$ electronic transitions using the pumping wavelength of 980 nm. The emission spectra are correlated with respect to the sample film thickness.

There is the clear evidence that the emission intensity increases with the decreasing refractive index and the increasing optical band gap energy, E_g. While the usual trend is that the emission intensity increases with the increasing refractive index because of promoting the radiative recombination probability. Sometimes, reabsorption processes may lead to such a reverse tendency [33,34] and this effect probably occurs in the cases of our samples studied.

In Fig. 3, we demonstrate that the photon up-conversion emission at pumping wavelength of 1 550 nm was distinctly observed only for sample **E**. The

Table I   Optical band gap energy, E_g, with error bar ±0.01 eV, film thickness, d, deposition time, t, and the deposition rate, DR, of pulsed laser Ga-Ge-Sb-S: Er^{3+} deposited films. The mean squared error, MSE, of ellipsometric data fit shown in the last column

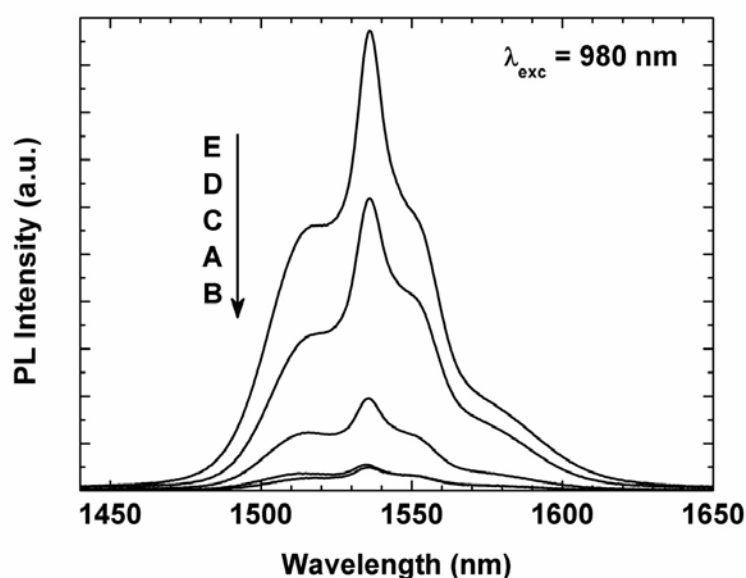| Sample	E_g eV	d nm	t min	DR nm min^{-1}	MSE
A	1.43	2 813 ± 4	95	29.6	8.892
B	1.44	1 546 ± 2	65	23.8	6.895
C	1.53	1 986 ± 2	95	20.9	6.596
D	1.75	2 600 ± 3	95	27.4	6.578
E	1.89	2 599 ± 1	100	26	8.395

Fig. 2   Stokes PL emission spectra of Ga-Ge-Sb-S: Er3+ pulsed laser deposited films normalised to their thickness. Excitation wavelength λ_{exc} = 980 nm and the emission band at $\lambda \approx 1.5$ μm originating from Er^{3+}: $^4I_{13/2} \rightarrow {}^4I_{15/2}$ electronic transitions

weak emission band was noticed at ≈ 995 nm, which is the signature of Er^{3+}: $^4I_{13/2} \rightarrow {}^4I_{15/2}$ electronic transitions. The experimental emission data of this sample were smoothed by the Savitzky–Golay filter [35] in order to increase the overall signal-to-noise ratio. The points of window for Savitzky–Golay filter were set to be 15 by using the polynomial function of the second order for smoothing process. Moreover, one can also observe an extremely weak signal ≈ 0.99 μm up-conversion emission in the sample **D** due to low signal-to-nise ratio; see Fig. 3. This observation is in agreement with the optical band gap energy values, E_g, of studied PLD samples varying from . 1.43 to 1.89 eV in wavelengths . 867-656 nm and in energy . 11 500-15 200 cm^{-1} for better understanding of the Er^{3+} energy
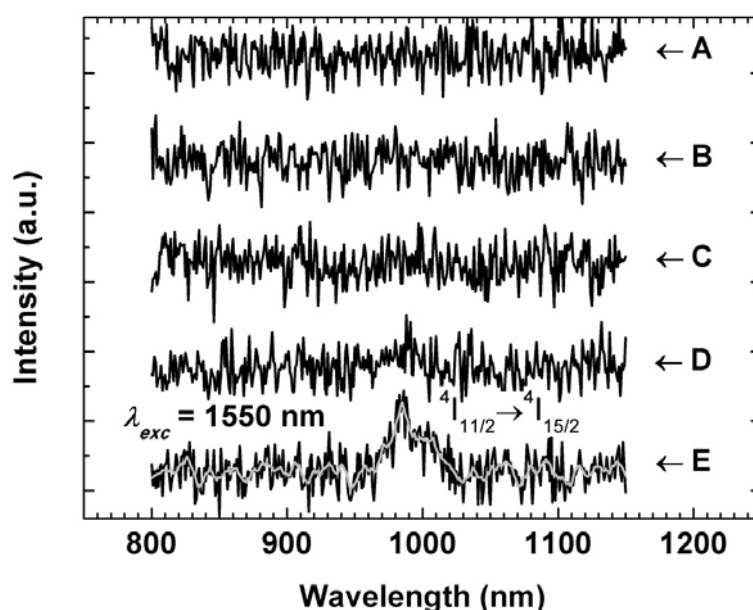
Fig. 3 Anti-Stokes PL emission spectra of Ga-Ge-Sb-S: Er3+ pulsed laser deposited films. Excitation wavelength λ_{exc} = 1 550 nm and the emission band at $\lambda \approx 990$ nm originating from Er^{3+}: $^4I_{11/2} \rightarrow {}^4I_{15/2}$ electronic transitions. The measured data of sample **E** smoothed using Savitzky–Golay filter (gray line)
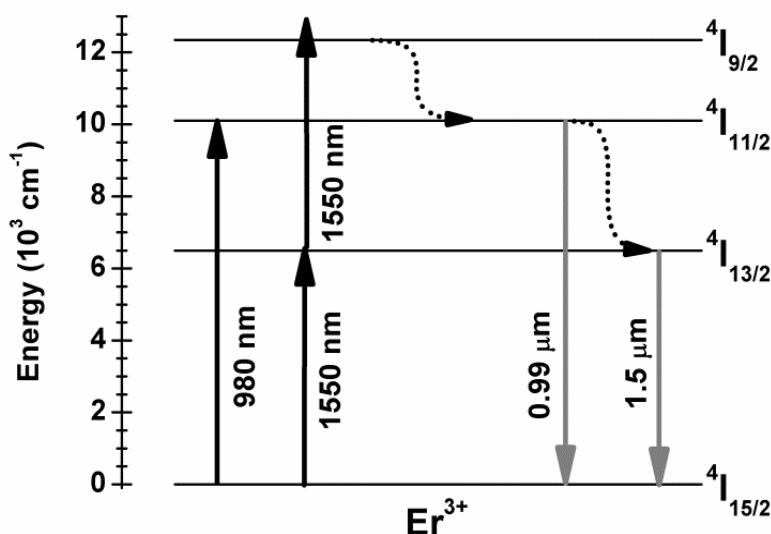

Fig. 4 Energy level diagram of Er^{3+} ion. Black arrows show the used pumping wavelengths, gray arrows highlight the observed emissions, and dotted black arrows represent the possible multiphonon relaxation processes in the Ga-Ge-Sb-S: Er^{3+} PLD films

level diagram in Fig. 4. The electron population of Er^{3+}: $^4I_{9/2}$ energy level is the essential process to obtain the photon up-conversion emission at pumping wavelength of 1 550 nm (see Fig. 4.). However, the optical band gap energies of samples **A**, **B**, **C** are too low to be able to populate the Er^{3+}: $^4I_{9/2}$ energy level (the energy $\approx 12 350$ cm^{-1}) by two-photon absorption with the mentioned pumping

Střižík L. *et al.*/Sci. Pap. Univ. Pardubice, Ser. A **21** (2015) 57–66

63

laser and under the absence of the emission from Er^{3+}: $^4I_{11/2} \rightarrow {}^4I_{15/2}$ transitions. The possible "Er^{3+}: $^4I_{13/2} \rightarrow$ chalcogenide $\rightarrow Er^{3+}$: $^4I_{11/2}$" interaction in these up-conversion processes potentially promoting the radiative recombination play probably negligible role.

The shape of photon up-conversion emission of the PLD film sample **E**; i.e., the $(Ge_{17.8}Ga_{3.6}Sb_{3.6}S_{75})_{99.5}Er_{0.5}$ structure, was compared with that of the sample **A**, i.e., $(Ge_{25}Ga_5Sb_5S_{65})_{99.5}Er_{0.5}$ bulk sample (see Fig. 5.). It is important to emphasise that the sample **E** could not be prepared in the amorphous form (as the bulk) *via* the melt-quenching technique and we had to select the bulk sample **A** as reference one, containing the same atomic ratios of cations as the sample **E**. It is obvious from Fig. 5 that the shapes of both up-conversion emission bands are similar to the same peak value to be centred at $\lambda \approx 985$ nm. The broader emission band in the PLD film sample was probably affected by higher noise level.
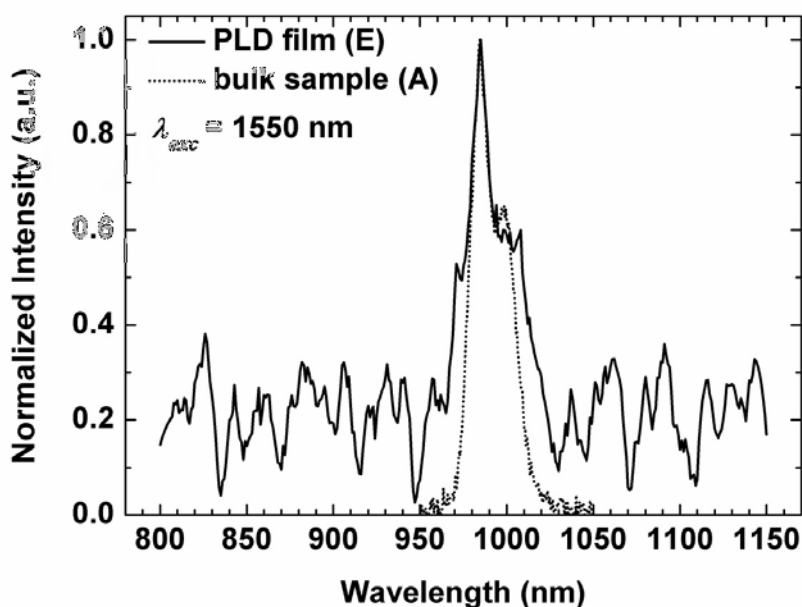

Fig. 5 Comparison of anti-Stokes PL emission spectra between $(Ge_{17.8}Ga_{3.6}Sb_{3.6}S_{75})_{99.5}Er_{0.5}$ **E** pulsed laser deposited film and the $(Ge_{25}Ga_5Sb_5S_{65})_{99.5}Er_{0.5}$ bulk sample. The spectrum of **E** film smoothed by Savitzky–Golay filter. Excitation wavelength $\lambda_{exc} = 1\,550$ nm and the emission band at $\lambda \approx 990$ nm originating from the Er^{3+}: $^4I_{11/2} \rightarrow {}^4I_{15/2}$ electronic transitions

Conclusion

In this article, we have presented the compositional dependence of Ga-Ge-Sb-S: Er^{3+} pulsed laser deposited films on the optical constants, the optical band gap energy, E_g, and photoluminescence emission at $\lambda \approx 1.5$ µm. It seems that the sulphur content should be kept high as much as possible in order to achieve maximally intensive emission band at $\lambda \approx 1.5$ µm originating from Er^{3+}:

$^4I_{13/2} \rightarrow {}^4I_{15/2}$ electronic transitions. The photon up-conversion emission band has been observed only for the PLD films with the highest amount of sulphur (75 at. %), i.e., $(Ge_{17.8}Ga_{3.6}Sb_{3.6}S_{75})_{99.5}Er_{0.5}$, by using the pumping wavelength of $\lambda \approx 1\,550$ nm. The emission was observed at $\lambda \approx 0.99$ μm being assigned to the Er^{3+}: $^4I_{11/2} \rightarrow {}^4I_{15/2}$ electronic transitions. Finally, a further improvement of the photon up-conversion emission intensity can be expected when glass-ceramics or photonic crystal structure on the surface of films are prepared and, in this respect, the chalcogenide PLD films have some promise as the material of choice for waveguides and sensors.

Acknowledgement

References

[1]   Kenyon A.J.: Prog. Quant. Electron. **26**, 225 (2002).

[2]   Zakery A., Elliott S.R: J. Non-Cryst. Solids **330**, 1 (2003).

[3]   Rode A.V., Zakery A., Samoc M., Charters R.B., Gamaly E.G., Luther-Davies B.: Appl. Surf. Sci. **197-198**, 481 (2002).

[4]   Prudenzano F., Mescia L., Allegretti L., Moizan V., Nazabal V., Smektala F.: Opt. Mater. **33**, 241 (2010).

[5]   Prudenzano F., Mescia L., Allegretti L.A., De Sario M., Palmisano T., Smektala F., Moizan V., Nazabal V., Troles J.: J. Non-Cryst. Solids **355**, 1145 (2009).

[6]   Tverjanovich A., Grigoriev Y.G., Degtyarev S.V., Kurochkin A.V., Man'shina A.A., Ivanova T.Y., Povolotskiy A., Tveryanovich Y.S.: J. Non-Cryst. Solids **326-327**, 311 (2003).

[7]   da Silva C.J., de Araujo M.T.: Opt. Mater. **22**, 275 (2003).

[8]   Lenth W., Macfarlane R.M.: Opt. Photonics News **3**, 8 (1992).

[9]   Le Person J., Colas F., Compère C., Lehaitre M., Anne M.L., Boussard-Plédel C., Bureau B., Adam J.L., Deputier S., Guilloux-Viry M.: Sensor. Actuat. B-Chem. **130**, 771 (2008).

[10] Charpentier F., Bureau B., Troles J., Boussard-Pledel C., Michel-Le Pierres K., Smektala F., Adam J.-L.: Opt. Mater. **31**, 496 (2009).

[11] Tanaka K., Shimakawa K.: *Amorphous Chalcogenide Semiconductors and Related Materials*, Springer, New York, 2011.

[12] Fairman R., Ushkov B.: *Semiconducting Chalcogenide Glass III: Applications of Chalcogenide Glasses*, Elsevier Inc., San Diego, 2004.

[13] Troles J., Niu Y., Duverger-Arfuso C., Smektala F., Brilland L., Nazabal V., Moizan V., Desevedavy F., Houizot P.: Mater. Res. Bull. **43**, 976 (2008).

[14] De Sario M., Mescia L., Prudenzano F., Smektala F., Deseveday F., Nazabal V., Troles J., Brilland L.: Opt. Laser Technol. **41**, 99 (2009).

[15] Nazabal V., Němec P., Jurdyc A. M., Zhang S., Charpentier F., Lhermite H., Charrier J., Guin J.P., Moreac A., Frumar M., Adam J.L.: Thin Solid Films **518**, 4941 (2010).

[16] Ichikawa M., Wakasugi T., Kadono K.: J. Non-Cryst. Solids **356**, 2235 (2010).

[17] Střižík L., Zhang J., Wágner T., Oswald J., Kohoutek T., Walsh B.M., Přikryl J., Svoboda R., Liu C., Frumarová B., Frumar M., Pavlišta M., Park W.J., Heo J.: J. Lumin. **147**, 209, (2014).

[18] Moizan V., Nazabal V., Troles J., Houizot P., Adam J.-L., Doualan J.-L., Moncorgé R., Smektala F., Gadret G., Pitois S., Canat G.: Opt. Mater. **31**, 39 (2008).

[19] Ichikawa M., Ishikawa Y., Wakasugi T., Kadono K.: Opt. Mater. **35**, 1914 (2013).

[20] Guimond Y., Adam J.-L., Jurdyc A.-M., Ma H.L., Mugnier J., Jacquier B.: J. Non-Cryst. Solids **256-257**, 378 (1999).

[21] Ren J., Wágner T., Oswald J., Orava J., Frumarová B., Frumar M.: J. Phys. Chem. Solids **71**, 30 (2010).

[22] Charpentier F., Starecki F., Doualan J. L., Jóvári P., Camy P., Troles J., Belin S., Bureau B., Nazabal V.: Mater. Lett. **101**, 21 (2013).

[23] Maharana P.K. Jha R.: Sensor. Actuat. B-Chem. **169**, 161 (2012).

[24] Jellison G.E. Modine F. A.: Appl. Phys. Lett. **69**, 371 (1996).

[25] Jellison G.E., Modine F.A.: Appl. Phys. Lett. **69**, 2137 (1996).

[26] Bruggemann D.A.G.: Ann. Phys. **24**, 636 (1935).

[27] Krbal M., Wágner T., Kohoutek T., Němec P., Orava J., Frumar M.: J. Phys. Chem. Solids **68**, 953 (2007).

[28] Wágner T., Krbal M., Jedelský J., Vlček M., Frumarová B., Frumar M.: J. Opt. Adv. Mater. **7**, 153 (2005).

[29] Wágner T., Krbal M., Němec P., Frumar M., Wagner T., Vlček M., Peřina V., Macková A., Hnatovitz V., Kasap S.O.: Appl. Phys. A-Mater. **79**, 1563 (2004).

[30] Moss T.S.: Phys. Status Solidi B **131**, 415 (1985).

[31] Clausius R.: *Die Mechanishe Wärmlehre*, Vieweg-Verlag, Brunswick, 1879.

[32] Mossotti O.: Mem. e Fisica di Modena **24**, 49 (1850).

[33] Hehlen M.P.: OSA Trends Opt. Photo. **1**, SM16 (1996).

[34] Koughia C. and Kasap S.O.: Opt. Express **16**, 7709 (2008).

[35] Savitzky A., Golay M.J.E.: Anal. Chem. **36**, 1627 (1964).